Energy Sources, Part A

ISSN: 1556-7036 (Print) 1556-7230 (Online) Journal homepage: https://www.tandfonline.com/loi/ueso20

Source Functions in Early Time Pressure Transient Analysis

S. Y. Pan , G. V. Chilingar & Z. S. Lin

To cite this article: S. Y. Pan , G. V. Chilingar & Z. S. Lin (2007) Source Functions in Early Time Pressure Transient Analysis, Energy Sources, Part A, 29:11, 961-982, DOI: 10.1080/15567030701198657

To link to this article: https://doi.org/10.1080/15567030701198657

Published online: 19 Jun 2007.

Energy Sources, Part A, 29:961–982, 2007

ISSN: 1556-7036 print/1556-7230 online
DOI: 10.1080/15567030701198657

Source Functions in Early Time Pressure Transient Analysis

S. Y. PAN

Department of Resources Engineering
National Cheng Kung University
Taiwan

G. V. CHILINGAR

Professor of Petroleum and Civil Engineering
University of Southern California
Los Angeles, California, USA

Z. S. LIN

Department of Resources Engineering
National Cheng Kung University
Taiwan

Abstract *The pressure responses of a reservoir can be obtained by convolving source functions and flow rates. Although the literature reports on deriving source functions analytically from the diffusivity equation, there is no study on deriving source functions using flow rates and pressure responses obtained from pressure transient tests. We therefore wanted to develop a methodology for obtaining the formation source functions using pressure data when pressure and flow-rate data are known. In addition, we wanted to study the characteristics of some source functions both from simulated data and from analytical methods in the literature.*

We demonstrate that the pressure functions (solutions of the diffusivity equation) of a test well can be calculated by convolving flow rates with source functions, and that the source functions can be derived by deconvoluting the pressure drop and flow rates available from the pressure-test data. Pressure function, flow rate, or source function can be obtained when two of these three functions are known. A source function (in time domain) with the wellbore storage effect is a horizontal line in a very early time and coincides with the infinite line source function or the infinite surface cylinder source function after the end of the wellbore storage effect. The source functions are almost the same for different positive skin factors. For a negative skin factor, a source function is initially a horizontal line and subsequently coincides with the infinite line source or infinite surface cylinder source functions.

Keywords boundary condition, convolution, deconvolution, skin effect, solution of diffusivity equation, wellbore storage

Address correspondence to Zsay-Shing Lin, Dept. of Resources Engineering, National Cheng Kung University, No. 1 University Road, Tainan 701, Taiwan. E-mail: zsaylin@mail.ncku.edu.tw

1. Introduction

The diffusivity equation that describes fluid flow in a porous medium under special boundary conditions and an initial condition can be solved analytically using the Laplace transform (Theis, 1935; van Everdingen and Hurst, 1949; Rosa and Horne, 1996), the Fourier transform (Andre and Bennion, 1970), or Green's function (Gringarten and Ramey, 1973; Rosa and Horne, 1996). The Theis (or line source) solution (Theis, 1935; Lee, 1982) is derived by assuming the intersection of the vertical well and formation to be a line source. The Theis solution is a special case of the van Everdingen and Hurst solution (1949), which includes cases with a constant flow rate and constant pressure and with finite and infinite reservoir sizes for outer boundary conditions.

Gringarten and Ramey (1973) used Green's function to solve the diffusivity equation. The integral of an instantaneous Green's function around an area with a special boundary condition is called a *source function*. Gringarten and Ramey (1973) derived several basic source functions, such as an infinite plane source function, infinite slab source function, infinite line source function, infinite surface cylinder source function, point source function, etc. From these basic source functions, they used Newman's product method to find more solutions of the diffusivity equation for different inner and/or outer boundary conditions. Clonts and Ramey (1986) presented an analytical pressure solution for a uniform flux horizontal drainhole in an anisotropic reservoir with finite thickness. In using source functions and the Newman product method, they found that the pressure solution of a uniform flux vertical fracture could be approximated by a vertical array of drainholes. Kuchuk et al. (1990) used deconvolution methods to compute the pressure behavior of a well/reservoir system from a well producing at a constant flow rate. They called the computed pressure behavior of the system *deconvolved pressure*. Later, Kuchuk (1990) utilized convolution and deconvolution interpretation methods to show that the downhole flow rate is crucial for system identification and parameter estimation. He also showed that the generalized rate convolution method worked better than the Horner method (Lee, 1982).

Different source functions represent different formation characteristics and/or different boundary conditions. By knowing the source function of a specific well, an appropriate model can be chosen to analyze the pressure data, and correct results will be obtained.

The purposes of this study were to obtain the formation source functions from pressure test data with pressure and flow-rate data taken from field data and simulation data to study the characteristics of source functions and to generate transient pressure information from source functions and flow-rate data. From the obtained formation source functions, the relationship of the test formation to differential boundary conditions is then revealed.

2. Basic Theory

2.1. Pressure Solutions of Diffusivity Equation

In deriving the diffusivity equation for radial flow toward a well in a circular reservoir, the isothermal flow of fluid with small and constant compressibility is assumed. The pressure gradient is assumed to be very small and the reservoir is assumed to be homogeneous and isotropic. All parameters of rock and fluid properties are assumed to be constant. By combining the conservation of mass and Darcy's law, the diffusivity equation in dimensionless form can be written as follows (Lee, 1982):

$$\frac{\partial^2 P_D}{\partial r_D^2} + \frac{1}{r_D}\frac{\partial P_D}{\partial r_D} = \frac{\partial P_D}{\partial t_D} \tag{1}$$

where

$$P_D = \frac{kh(P_i - P_{wf})}{141.2 q \mu B} \quad \text{for oil} \tag{2}$$

$$P_D = \frac{kh(P_i^2 - P_{wf}^2)}{1{,}422 q \mu Z T} \quad \text{for gas} \tag{3}$$

$$t_D = \frac{0.0002637 kt}{\phi \mu C r_w^2} \tag{4}$$

$$r_D = r/r_w \tag{5}$$

By giving initial and boundary conditions, the solution of the diffusivity equation can be derived analytically, semi-analytically, or numerically. These solutions include the van Everdingen and Hurst solution (van Everdingen and Hurst, 1949), the Theis solution (Theis, 1935), and the log approximation solution (Lee, 1982). In addition, the solutions of the diffusivity equation can also be solved using known source functions and flow rates (Gringarten and Ramey, 1973).

2.2. Source Function Solutions and Convolution

Some of the solutions of the diffusivity equation, or the pressure response function ($P_D(t_D)$) can be derived by convolving source functions ($S(t_D)$) with flow rates ($q_D(t_D)$) (Gringarten and Ramey, 1973; Raghavan, 1993):

$$P_D(t_D) = q_D(t_D) * S(t_D) = \int_0^{t_D} q_D(\tau) S(t_D - \tau)\, d\tau \tag{6}$$

where "$*$" is the operator of convolution.

The convolution method is used to filter data in signal processing, and the relationships among pressure response ($P_D(t_D)$), flow rate ($q_D(t_D)$), and formation characteristic ($S(t_D)$) comprise a filter system (Figure 1) in which flow rate is the input, pressure response is the output, and the formation source function is the filter. Because the filter system is a linear system, the pressure response is the convolution of a flow rate and source function, which is based on Eq. (6).

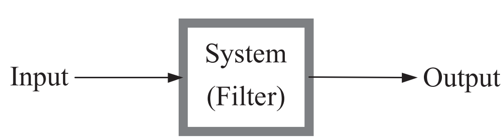

Figure 1. The linear system that is constructed using an input, filter, and output.

The pressure, flow rate, and source function in Eq. (6) are continuous functions. In numerical calculations, the pressure, flow rate, and source function are discrete. When the flow rate and source function comprise N values in the time domain, a discrete equation (Eq. (7)) can be used to calculate the convolution result of both (Oppenheim et al., 1999).

$$P_D^*[n'] = q_D[n] * S[n] \equiv \sum_{m=0}^{N-1} q_D[m]S[n-m] \tag{7}$$

where $n = 0, 1, 2, \ldots, N-1$ and $n' = 0, 1, 2, \ldots, 2N-2$.

In the convolution method, the q_D function is stationary, and the S function in Eq. (7) first mirrors or folds from the y-axis in Cartesian coordinates and then moves rightward until the last point of S dislocates the range of q_D. When the S function is moving rightward by steps, the summations of the products of S and q_D in each step are formed as the result of the linear convolution shown in Eq. (7) (Oppenheim et al., 1999).

Notice that P_D^* is the result of the linear convolution of q_D and S, and the length of P_D^* is $2N-1$. If the q_D and S functions are known, the linear convolution of q_D and S can be calculated from Eq. (7). But the solution of the diffusivity equation, $P_D(t_D)$, is the first N points of the linear convolution, and the posterior $N-1$ points are discarded. These solutions derived from source functions are also called *source function solutions*.

2.3. Source Function using the Deconvolution Method

To compute the source function (S) when the P_D and q_D functions are known from Eq. (6) or Eq. (7) the length of the pressure function should be $2N-1$, where the lengths of q_D and S are N. It is necessary to pad zeros and make the length of the pressure data (P_D) be $2N-1$ points before the deconvolution process. Then the source function can be estimated by deconvolution (MATLAB, 2000), based on Eq. (7), as follows:

Step 1. Zero-padding $P_D[n]$, letting the length of $P_D[n]$ be $2N-1$.
Step 2. Using Eq. (7) to deconvolute $P_D^*[n']$ and $q_D[n]$ to obtain the result of $S[n]$.

Unlike Raghavan's method (Raghavan, 1993), the source function (S) in Eq. (6) is calculated in this study from knowing P_D and q_D and using polynomial division. If the source function (S), pressure data (P_D), and flow rate (q_D) sequences constitute the coefficients of polynomial S_p, $(P_D)_p$, and $(q_D)_p$, the polynomial S_p is equivalent to the quotient when the polynomial $(P_D)_p$ is divided by the polynomial $(q_D)_p$. And the coefficients of the quotient, S_p, are equivalent to the source function sequences (S) (Eq. (8)) (MATLAB, 2000):

$$S_p = (P_D)_p/(q_D)_p \tag{8}$$

Notice that the source function sequences constitute the coefficients of S_p, as do the pressure and flow-rate data. From the polynomial division theorem, the quotient, S_p, exists when the degree of the dividend, $(P_D)_p$, is greater than or equals to the degree of $(q_D)_p$. Otherwise, there will be no quotient or the quotient is constant. The degree of P_D must be added to $2N-1$ to obtain the N degree of the quotient when the degrees of P_D and q_D are equal, i.e., N. The easiest way to expand the degree of a polynomial is by adding zeros to lower power items (MATLAB, 2000).

3. Results

The relationship of flow rates (q_D), source functions (S), and bottom hole pressure (P_D) in Eq. (6) can be viewed as the input (q_D, flow rates), filter (S, source functions), and output (P_D, the pressure drop) in a system (or formation) (Kuchuk et al., 1990; Kuchuk, 1990). The system is characteristically a linear system in which the superposition method can be used.

3.1. Source Functions and Their Characteristics

The basic source functions (Gringarten and Ramey, 1973), such as the point source function, $S_{ps}(t)$, infinite line source function, $S_{il}(t)$, and infinite surface cylinder source function, $S_{is}(t)$, are (Gringarten and Ramey, 1973):

$$S_{ps}(t) = \frac{e^{-r^2/4\eta_r t}}{8(\pi\eta_r t)^{3/2}} \tag{9}$$

$$S_{il}(t) = \frac{e^{-r^2/4\eta_r t}}{4\pi\eta_r t} \tag{10}$$

$$S_{is}(t) = \frac{r_w}{2\eta_r t} I_o\left(\frac{r r_w}{2\eta_r t}\right) e^{-(r^2+r_w^2)/4\eta_r t} \tag{11}$$

where

$$\eta_r = \frac{k}{\mu C\phi} \tag{12}$$

Point source is a well that is perforated in a formation with a very small interval as a point. Infinite line source is a well that is perforated in a formation with a finite interval where the diameter of the well is very small (approaches zero). In the infinite surface cylinder source, the diameter of the well does not approach zero. Dimensionless source functions corresponding to Eqs. (9) to (11) are written as:

$$S_{ps}(t_D) = \frac{1}{4\sqrt{\pi}t_D^{3/2}}\ e^{[\frac{-1}{4t_D}]} \tag{13}$$

$$S_{il}(t_D) = \frac{1}{2t_D}\ e^{[\frac{-1}{4t_D}]} \tag{14}$$

$$S_{is}(t_D) = \frac{1}{2t_D} I_o\left(\frac{1}{2t_D}\right) e^{[\frac{-2}{4t_D}]} \tag{15}$$

where

$$t_D = \frac{kt}{\mu C\phi r_w^2}$$

$$r_D = r/r_w \qquad (r_D = 1 \text{ at wellbore})$$

In a log-log plot, the infinite surface cylinder source function decreases as dimensionless time increases (Figure 2). The dimensionless point source function and dimensionless infinite line source function increase as dimensionless time increases in the early-time period. After reaching the maximum for t_D (approximately 0.11), both source functions decrease as dimensionless time increases. The point source function and infinite line source function coincide when t_D is between 10^{-2} and 10^{-1}. The infinite surface cylinder function, however, initially differs from these two functions when $t_D < 10^{-1}$ (Figure 2). Thus, the pressure behavior of the point source function and infinite line source function is the same in the flow period when t_D is between 10^{-2} and 10^{-1}. The infinite line source function is close to the infinite surface cylinder source function and different from the point source function when $t_D > 10^{-1}$. Therefore, the pressure behavior of the infinite line source function is the same as that of the infinite surface cylinder source function and different from that of the point source function when $t_D > 10^{-1}$.

3.2. Pressure Solutions from Source Functions

If source functions (Eqs. (13) to (15)) are used to solve the solutions of the diffusivity equation (Eq. (6)), pressure solutions (Eqs. (16) to (18)) corresponding to the point source function, infinite line source function, and infinite surface cylinder source function are obtained, such as,

$$P_{D,ps}(t_D) = q_D * S_{ps}(t_D) = q_D * \frac{1}{4\sqrt{\pi}t_D^{3/2}}\ e^{[\frac{-1}{4t_D}]} \tag{16}$$

$$P_{D,il}(t_D) = q_D * S_{il}(t_D) = q_D * \frac{1}{2t_D}\ e^{[\frac{-1}{4t_D}]} \tag{17}$$

$$P_{D,is}(t_D) = q_D * S_{is}(t_D) = q_D * \frac{1}{2t_D} I_o\left(\frac{1}{2t_D}\right) e^{[\frac{-2}{4t_D}]} \tag{18}$$

Notice that the pressure transient solution (P_D) is the first N points of the convolution of $q_D * S(t_D)$ where $S(t_D)$ may be either $S_{ps}(t_D)$, $S_{il}(t_D)$, or $S_{is}(t_D)$. For a constant flow rate ($q_D = 1$), the convolution method is used to obtain dimensionless pressure solutions (Figure 3) for the point source, infinite line source, and infinite surface cylinder source functions (Eqs. (16) to (18)). The infinite line source pressure transient solution, $P_{D,il}(t_D)$, and infinite surface cylinder source pressure transient solution, $P_{D,is}(t_D)$, are very consistent with the Theis solution and the van Everdingen and Hurst solution, respectively (Figure 4). These results show that the calculations of convolution in this study are correct.

The sampling rate or the dimensionless time interval will affect the results of calculations. For example, better results are obtained when a dimensionless time interval of 0.0705 is used to calculate the infinite surface cylinder source function and 0.015 is used to calculate the infinite line source function solution. The characteristics of the point source function and solution are not discussed in this study because there is no equivalent pressure solution available in the literature.

From the results shown above, the pressure solutions or pressure transient behavior can be obtained when the source functions of the formation and flow rates are known. Alternatively, the infinite line source function, the point source function, or the infinite surface cylinder source function can be obtained from Eq. (6) by deconvolving when the pressure solutions (P_D) and the flow rates are known. The infinite line source and infinite surface cylinder source functions calculated from deconvolution based on Eqs. (17) to (18) are the same as those from Eqs. (14) and (15) (Figure 5). These confirm that the

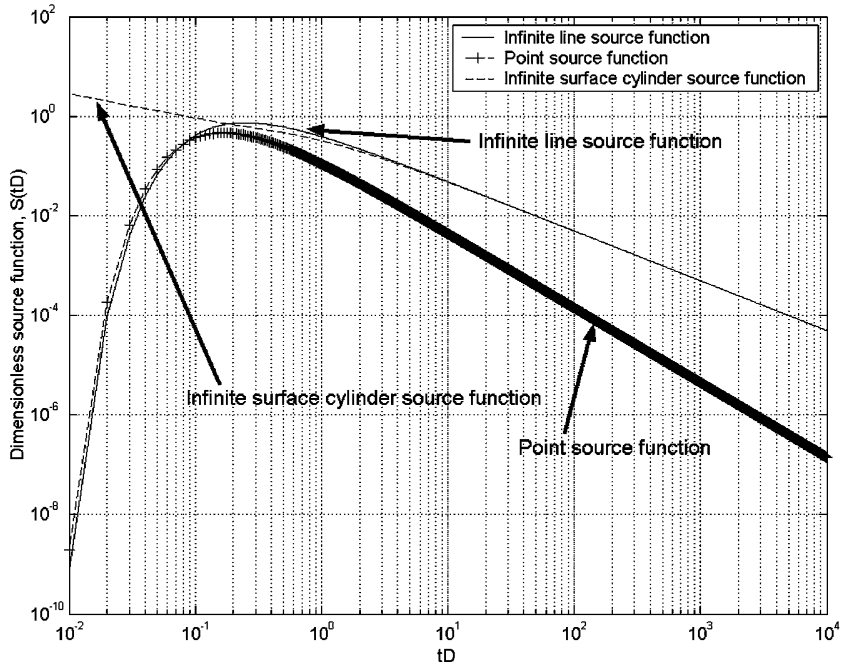

Figure 2. Characteristics of the infinite line, point, and infinite surface cylinder source functions.

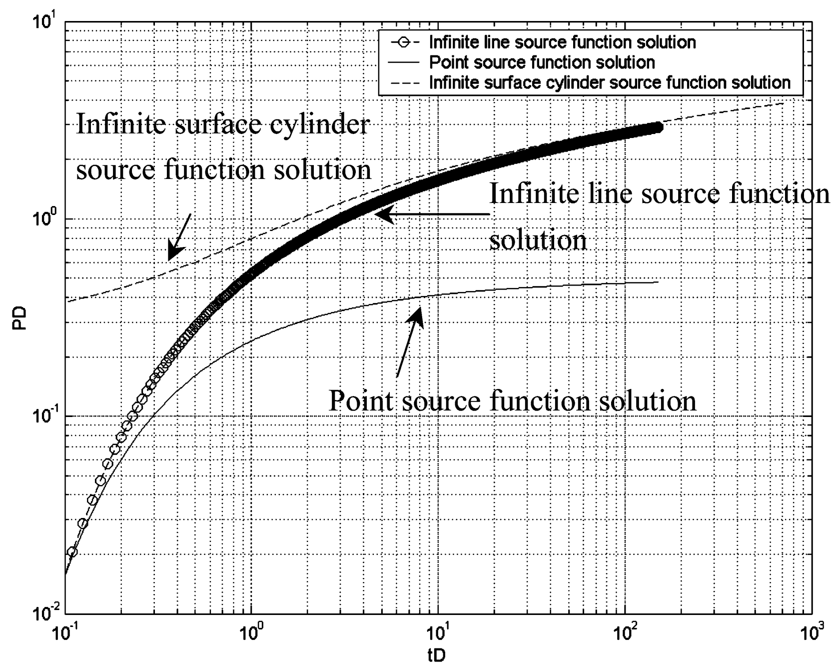

Figure 3. Diffusivity equation solutions derived from the infinite line, point, and infinite surface cylinder source functions.

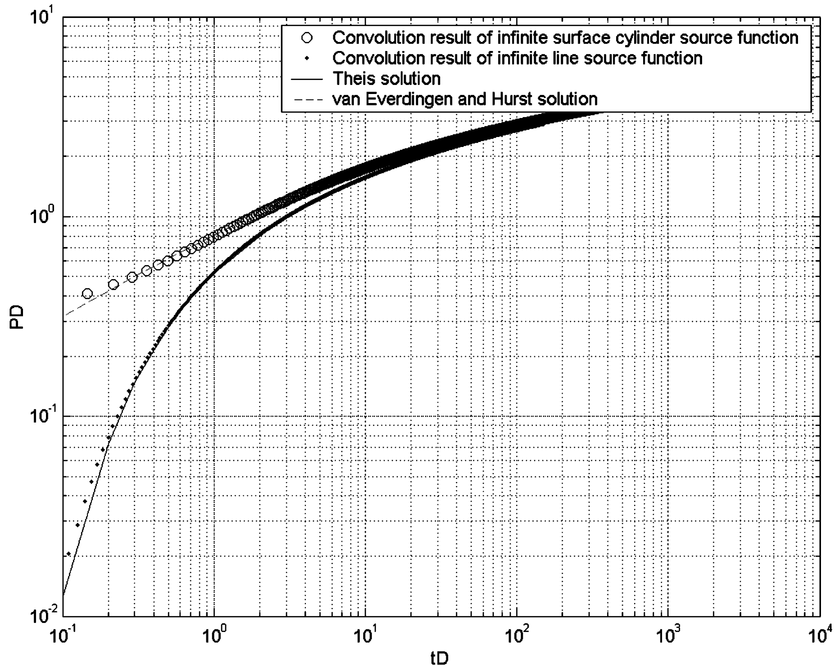

Figure 4. Comparison among the infinite line source function, the infinite surface cylinder source function solutions and the two analytical solutions.

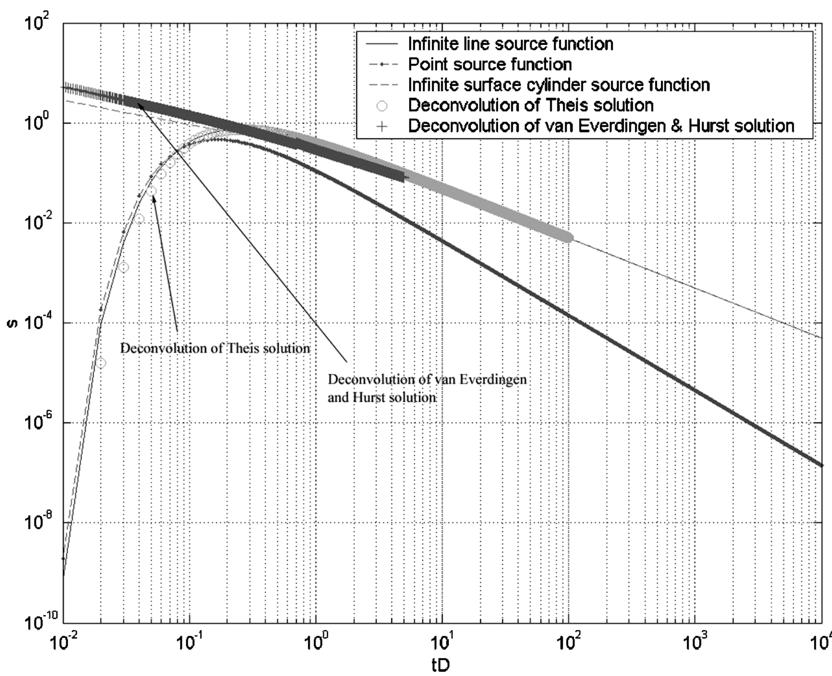

Figure 5. Comparison among the deconvolutions of the Theis solution, van Everdingen and Hurst solution, and the three analytical solutions.

deconvolution method of this study is correct. In addition, it is shown that the source functions can be obtained when the pressure functions and flow-rate data are known.

3.3. Formation Source Functions from Simulated Pressure Data

In this study, the IMEX simulator of Computer Modelling Group Ltd. (CMG, 2000) was used to construct a model (Table 1) and simulate pressure tests for an oil well in a radial flow for drawdown and buildup tests with the wellbore storage effect and skin effect. The goal was to obtain source functions from the pressure data generated by simulation.

3.3.1. Source Function from a Pressure Drawdown Test. The pressure data of a drawdown test with a constant flow rate (25 STB/DAY) (Figure 6) was obtained from the IMEX simulator. The dimensionless pressure from simulation is almost identical to the van Everdingen and Hurst solution (Figure 7), and the source function derived from deconvolution of pressure from simulation data under a constant flow rate is almost identical to the infinite surface cylinder source function (Figure 8). When the pressure drop (instead of dimensionless pressure) and the flow rate ($q = 25$ STB/DAY) for deconvolution are simulated, the corresponding source function can be obtained (Figure 9). Using the results shown in Figure 9, the dimensionless source function (Figure 10) can also be obtained. The relationship between the source function ($S(t)$) and dimensionless source function ($S(t_D)$) is shown in Eq. (19).

$$S(t) = \frac{0.8936B}{hC\phi r_w^2} S(t_D) \tag{19}$$

3.3.2. Source Function from a Pressure Buildup Test. The pressure buildup test data is simulated from the well being shut-in after producing a constant rate of 25 STB/DAY (Figure 11). The duration for both drawdown and buildup tests is 360 hrs. Based on the simulated pressure drop and flow rates (25 STB/DAY for pressure drawdown and 0 STB/DAY for pressure buildup), the source function ($S(t)$) is calculated using Eq. (7) (Figure 12). The dimensionless source function ($S(t_D)$), from using Eq. (19), matches with the infinite line source function or the infinite surface cylinder source function (Figure 13).

Table 1
Input parameters of the simulation for radial oil well

Parameters	Value, unit	Parameters	Value, unit
Permeability (k)	10 md	Viscosity for oil (μ)	13.2 cp
Porosity (ϕ)	0.17	Formation volume factor (B_{oil})	1.02 RB/STB
Thickness (h)	147 ft	Radius of well (r_w)	0.5 ft
Compressibility for oil (C_{oil})	$2 \cdot 10^{-6}$ psi^{-1}	Initial pressure (Pi)	3,200 psi
Compressibility for water (C_{water})	$2.6 \cdot 10^{-6}$ psi^{-1}	Initial oil saturation ($S_{\text{oil},i}$)	1
Compressibility for formation ($C_{\text{formation}}$)	10^{-8} psi^{-1}	Connate water saturation ($S_{\text{water},c}$)	0
Total compressibility (C_t)	$2 \cdot 10^{-6} + 10^{-8}$ psi^{-1}	Skin factor (s)	0

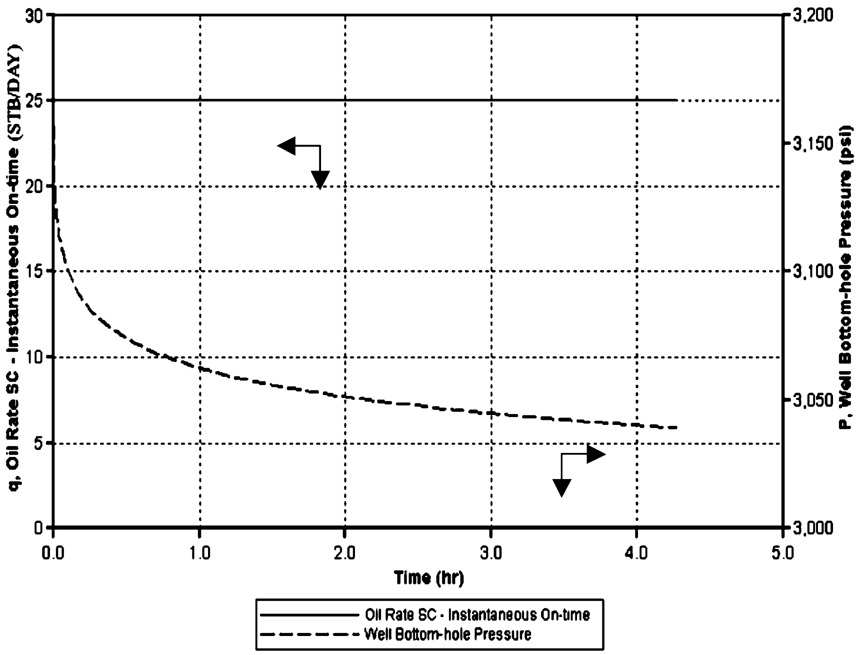

Figure 6. Pressure drawdown test simulated using the IMEX program.

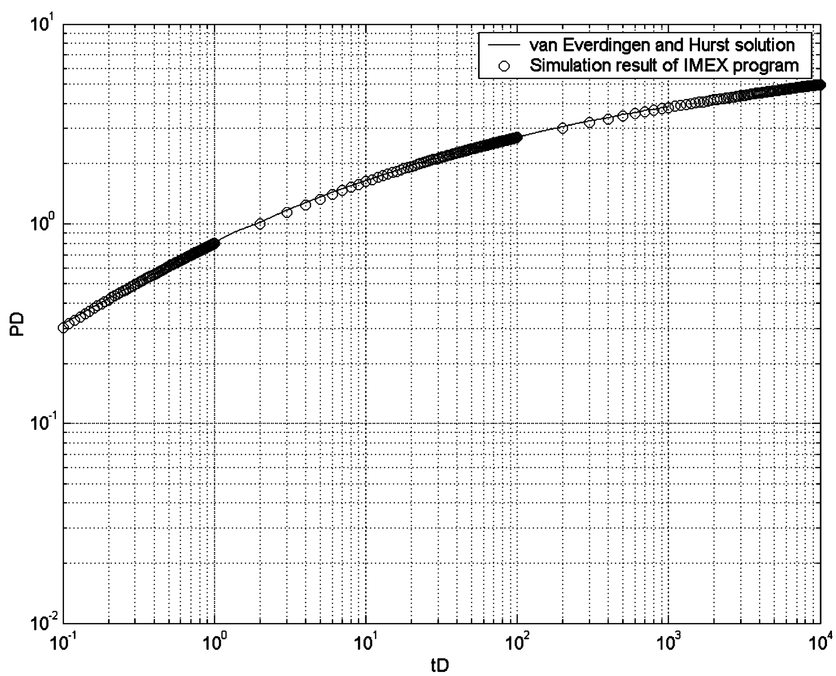

Figure 7. Comparison between the results from pressure drawdown data simulated using the IMEX program and from the van Everdingen and Hurst solution.

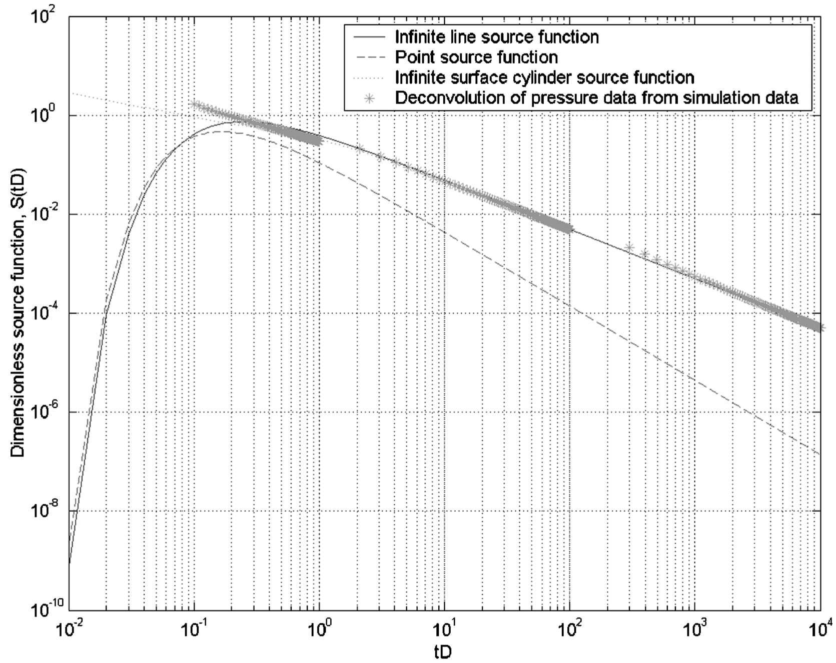

Figure 8. Comparison among the formation source function of pressure drawdown test simulated using the IMEX program and three analytical source functions.

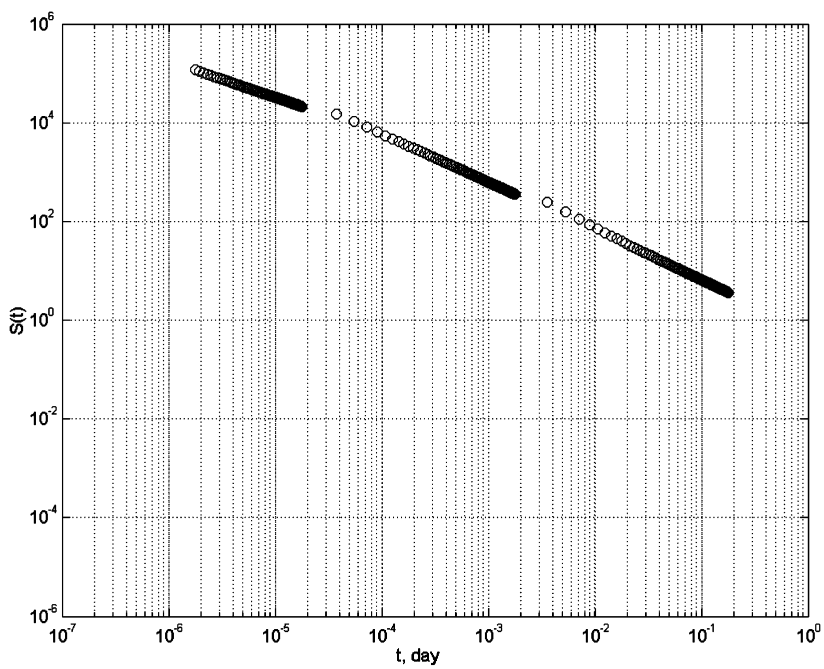

Figure 9. Source function obtained by deconvoluting ΔP and flow rate from simulated pressure drawdown test data.

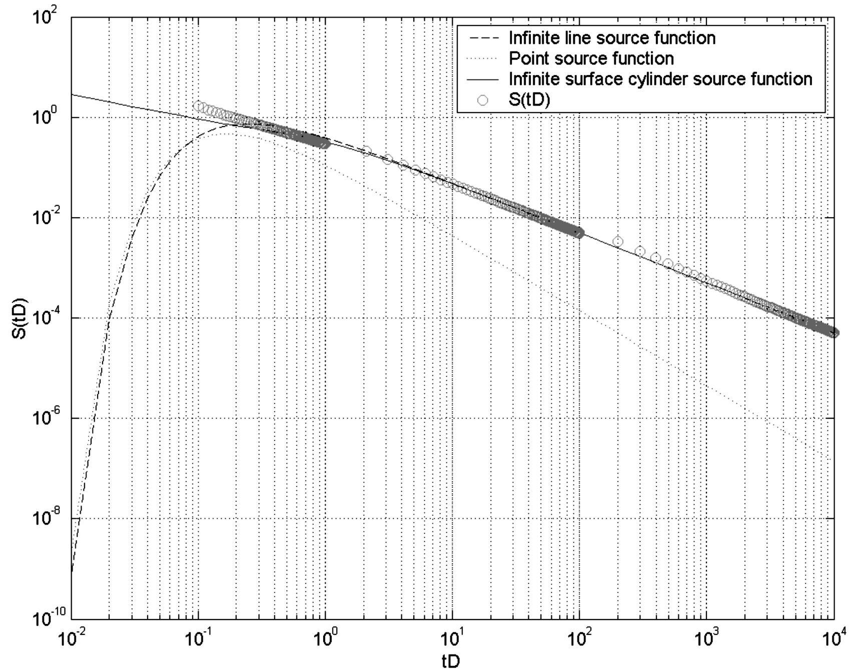

Figure 10. Dimensionless source function obtained from simulated pressure drawdown test data.

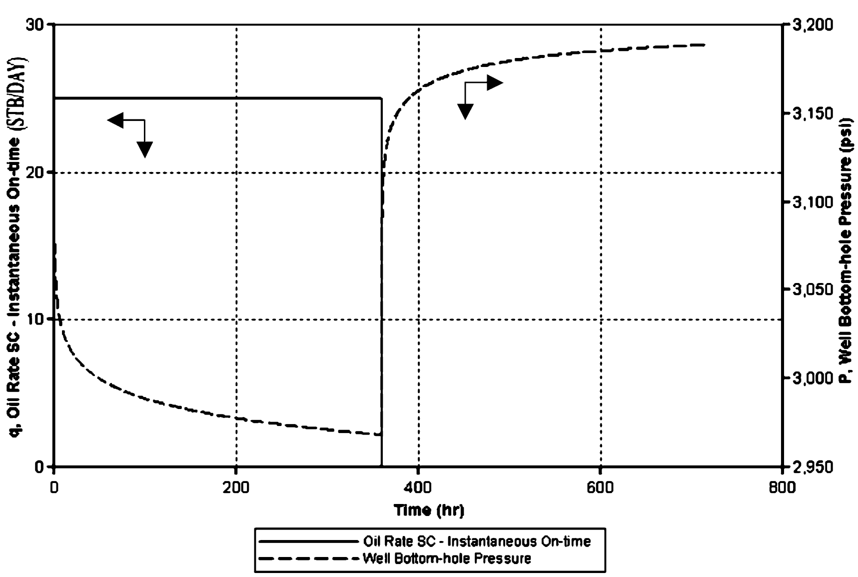

Figure 11. Pressure drawdown and buildup data simulated using the IMEX program.

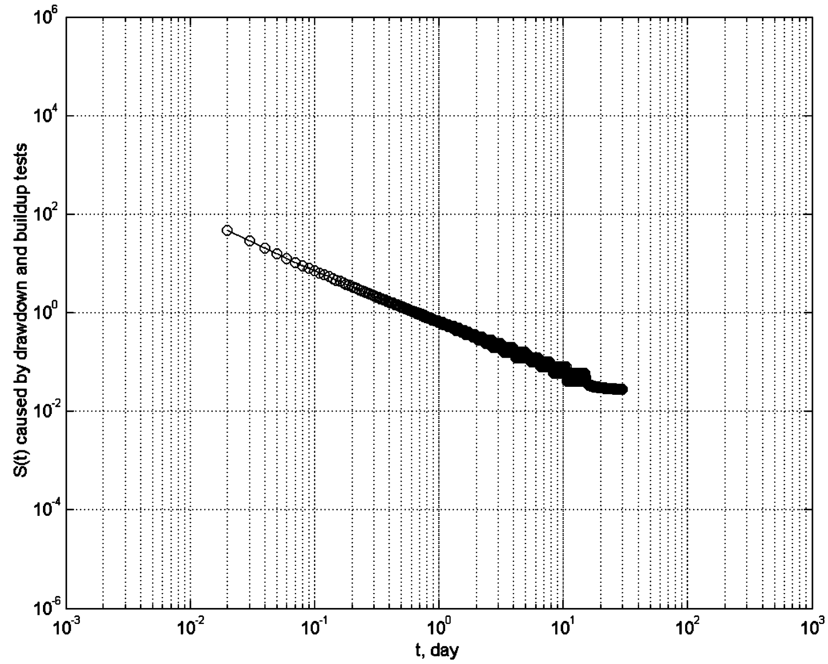

Figure 12. Source function obtained by deconvoluting ΔP and flow rate from simulated pressure drawdown and buildup tests ($q = 25$ and 0 STB/DAY).

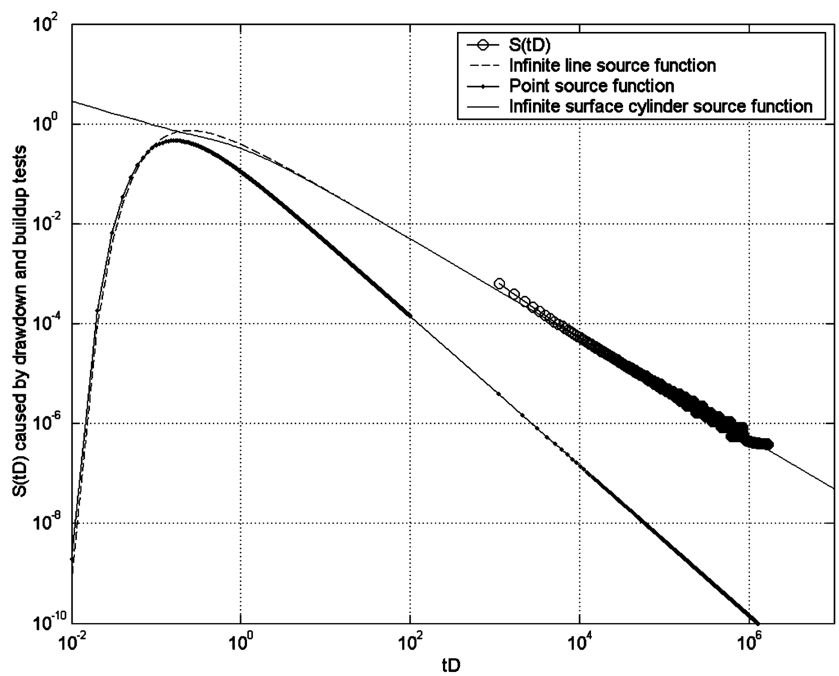

Figure 13. Dimensionless source function obtained from simulated pressure drawdown and buildup tests (q = 25 and 0 STB/DAY).

3.3.3. Source Functions with the Wellbore Storage Effect. There is no wellbore storage effect or skin effect in the simulation model discussed above. In the following example, wellbore pressure responses with the wellbore storage effect for the dimensionless wellbore storage constants ($C_D = 1$, 100, and 1,000) are simulated (Figure 14). The dimensionless wellbore storage constant ($C_D e^{2s} = 0.8936 C_c e^{2s} / C_t h r_w^2$) is defined by Bourdet et al. (1989).

Based on the simulated pressure, source functions (Figure 15) can be obtained using deconvolution of Eq. (6) or Eq. (7). Notice that a constant flow rate is used in these cases. When the dimensionless wellbore storage constant is small (such as $C_D = 1$), i.e., the wellbore storage volume is small, the source function is close to the infinite line source function or the infinite surface cylinder source function (Figure 15). When the dimensionless wellbore storage constant is larger (such as $C_D = 100$ or 1,000), the source function yields a horizontal line in a very early time. The larger the dimensionless wellbore storage constant is, the longer the horizontal line extends. The value of the source function decreases as the dimensionless wellbore storage constant increases (Figure 15). The horizontal line crosses the curve of the infinite surface cylinder source function and then coincides with the curve of the infinite surface cylinder source function at a later time. The coincident time is the ending time of the wellbore storage effect. The ending time (t_D) of the wellbore storage effect for the case studied is estimated at 4,000 when $C_D = 100$ and at 70,000 when $C_D = 1,000$ (Figure 15). These estimations are the same as those from the Ramey type-curve method (Lee, 1982) (Figure 16).

3.3.4. Source Functions with the Skin Effect. When simulating pressure test data with skin factors of 0, 2, 4, and 6 (damage effect), pressure data (Figure 17) is obtained to derive source functions with the skin effect (Figure 18). The source function without the skin effect ($s = 0$) from simulated data coincides with the infinite surface cylinder source function of the analytical solution (Figure 18a). The source functions for $s = 0$ and $s = 2$ are almost identical to each other when t_D is greater than 0.09 (Figure 18b). The source functions for $s = 0$ and $s = 4$ are consistent when t_D is greater than 0.12 (Figure 18c). The curve of each source function with a skin factor greater than zero deviates from the curve with a zero skin factor, and the initiation point of the deviation moves toward the right in the plot as the skin factor increases (Figure 18b and 18c). Because the skin effect occurs near the wellbore, the curve of a source function with a skin factor greater than zero tends to coincide with the infinite line source function or the infinite surface cylinder source function at a late time.

When simulating pressure test data with skin factors of −2, −4, or −6 (stimulation effect), pressure data (Figure 19) is obtained from simulation to derive source functions with the skin effect (Figure 20). The source function with a negative skin factor is similar to the source function with the wellbore storage effect, and it, too, produces a horizontal line at an early time. Moreover, for negative skin, as the value of the skin factor becomes smaller, the value of the source function of the horizontal line becomes smaller. A source function with a negative skin factor tends to coincide with the infinite surface cylinder source function or the infinite line source function at a later time. Nevertheless, unlike the source function with the wellbore storage effect, the source function curve with a negative skin factor does not cross the infinite surface cylinder source function curve or infinite line source function curve.

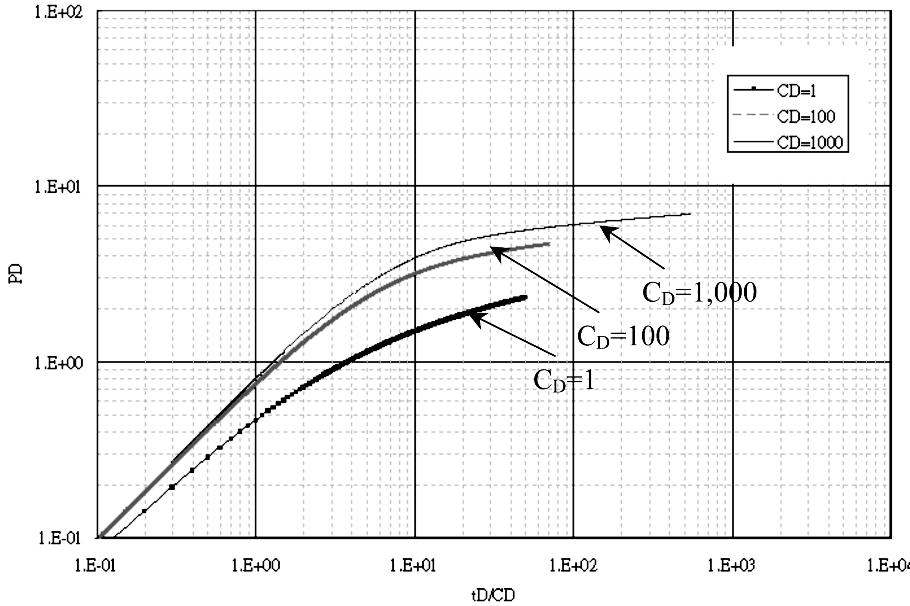

Figure 14. Pressure data simulated using the IMEX program for the wellbore storage effect.

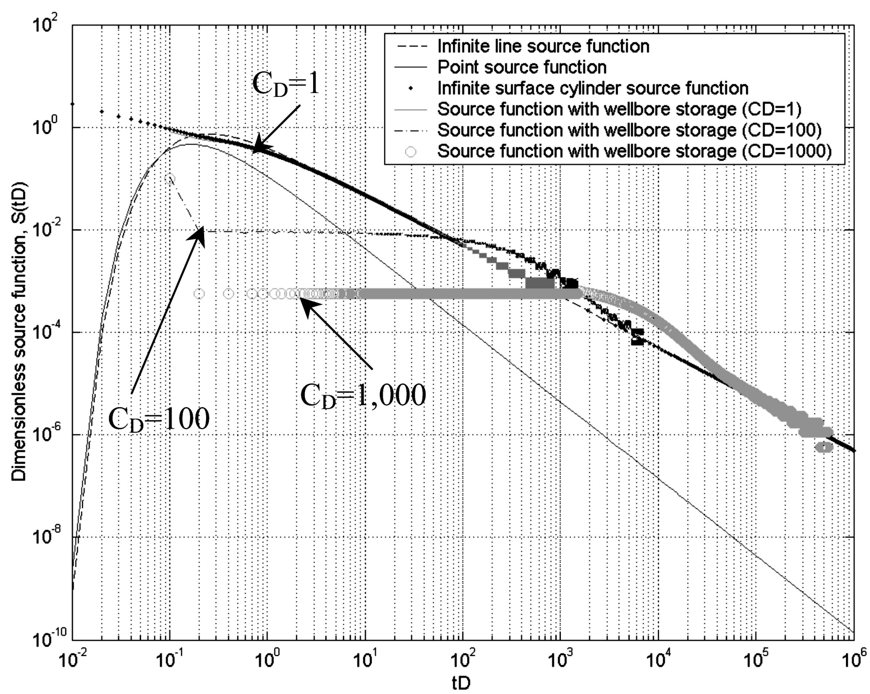

Figure 15. Comparison among the formation source functions caused by the wellbore storage effect and the three analytical source functions.

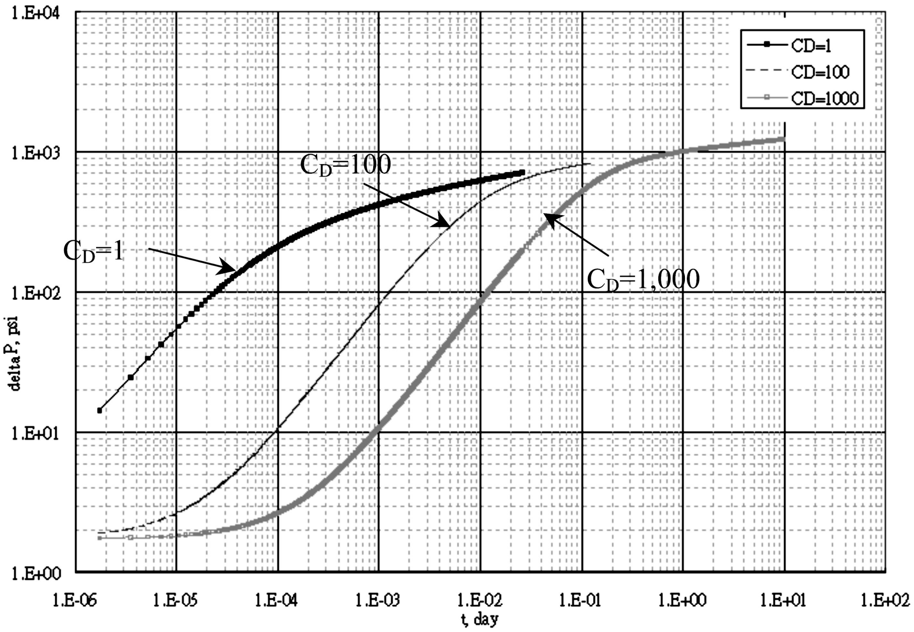

Figure 16. Traditional estimation of ending time for the wellbore storage effect.

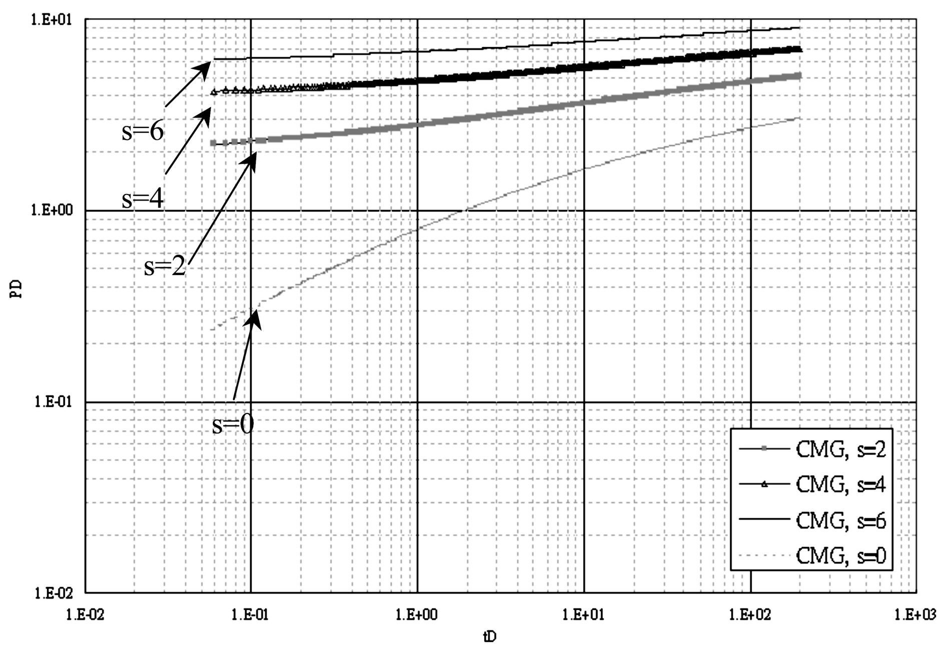

Figure 17. Pressure data simulated using the IMEX program for the skin effect ($s = 0, 2, 4, 6$).

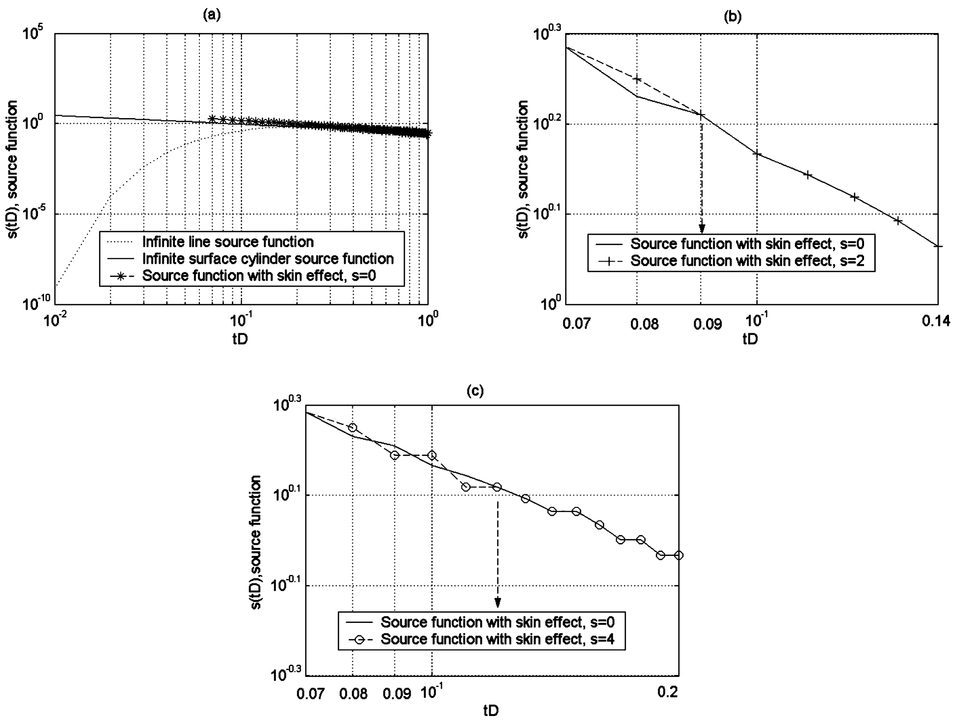

Figure 18. Comparison of source functions for different skin factors: (a) the source function for $s = 0$, infinite line source function, and infinite surface cylinder source function; (b) the source functions for $s = 0$ and 2; (c) the source functions for $s = 0$ and 4.

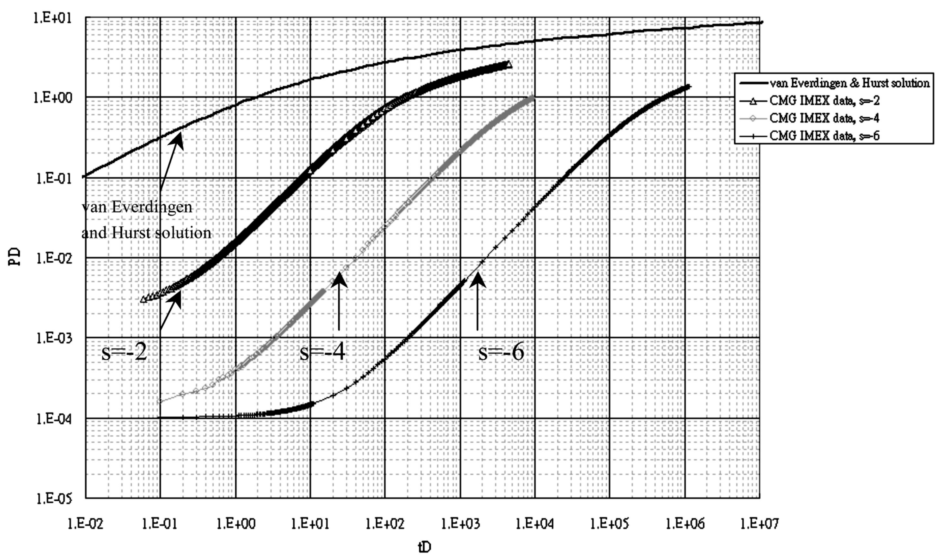

Figure 19. Pressure data simulated using the IMEX program for the skin effect ($s = -2, -4, -6$).

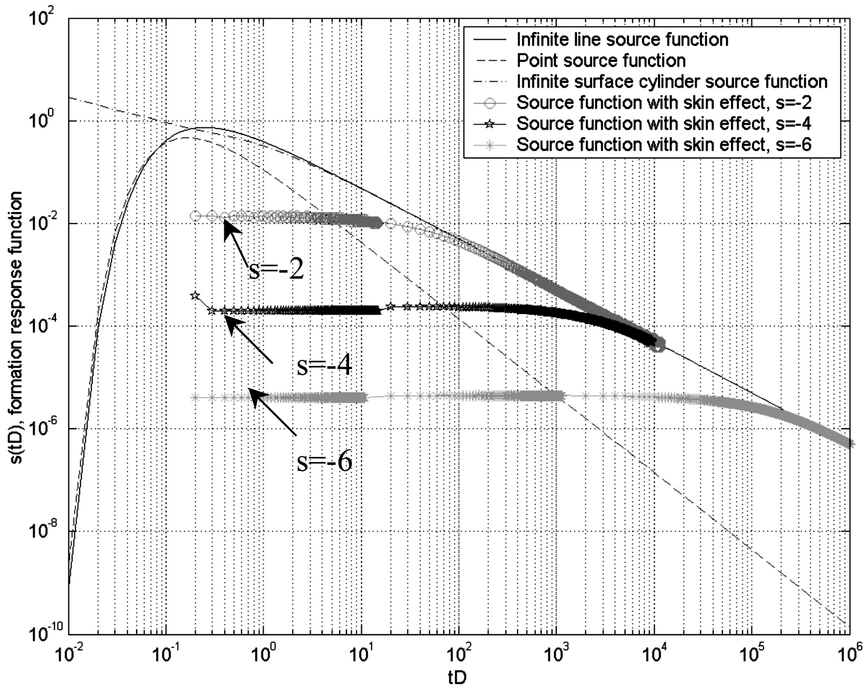

Figure 20. Comparison among the formation source functions caused by the skin effect and the three analytical source functions.

4. Discussions

(1) Based on one of the analytical solutions shown in Eq. (6), the formation is a linear system (Gringarten and Ramey, 1973; Kuchuk et al., 1990). Moreover, the linear system can be viewed as consisting of an input, $q_D(t_D)$, a filter, $S(t_D)$, and an output, $P_D(t_D)$ (Figure 1). The pressure drop (P_D) can be obtained by convoluting flow rates (q_D) and source functions (S) (Eq. (6)). If the pressure drop and flow rates are known, the source functions can be derived by deconvoluting the pressure drop and flow rates. In our study, the convolution and deconvolution methods were used regardless of whether or not the flow rates were constant.

(2) When simulated pressure and flow-rate data are provided, the deconvolution method, which is used in signal processing, can be used to obtain source functions. Our results show that these source functions are affected by the system or the boundary condition of a formation but not by flow rates, because the pressure response changes as the flow rate changes. Thus, the source functions depend only on the characteristics of the formation.

(3) The characteristics of the source functions are related to the boundary conditions. This study investigated the source functions affected by inner boundary conditions, especially a well's geometry or its intersection with the formation. In addition, the inner boundary conditions affect the early-time pressure test data. Because these source functions vary for different inner boundary conditions, they are affected by the wellbore storage effect and the skin effect. In our study, the source functions were clearly influenced by the wellbore storage effect. The source functions were more strongly affected

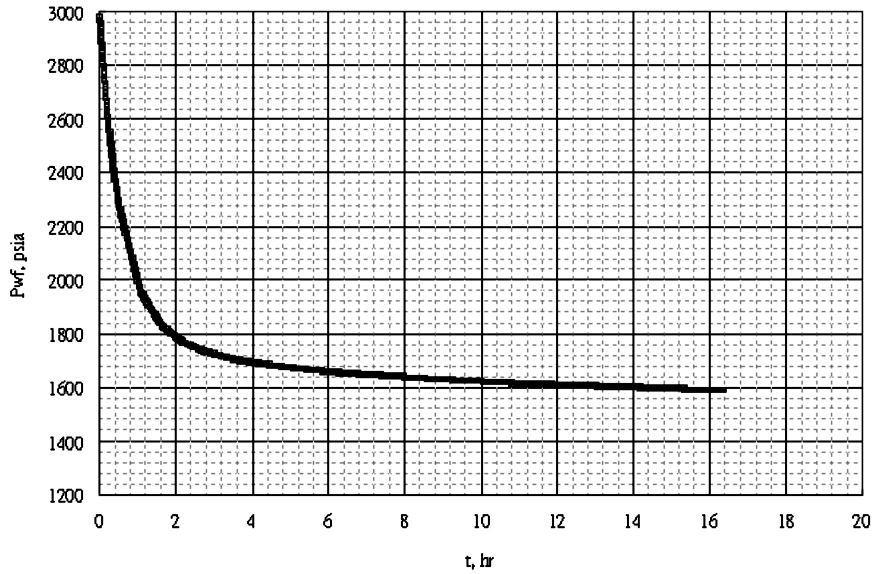

Figure 21. Pressure data in Lee (1982).

by negative skin factors (the stimulation effect) than by positive skin factors (the damage effect). The reason may be that the effective wellbore radius is very small when the skin factor is positive. Therefore, the damage effect was not apparent. The small fluctuation caused by the damage effect had to be observed in very small scale and may have been caused by numerical simulation. Moreover, the source function with the wellbore storage effect differed from the source function with the stimulation effect, and this difference can be used to distinguish the skin effect from the wellbore storage effect.

5. Case Study

The reservoir data for the case study is from the literature and contains pressure test data (Figure 21) and general information (Table 2). The pressure test (Figure 21) was a drawdown test from a well with the wellbore storage effect and skin effect. The dimensionless wellbore storage constant was 1,000, and the duration of the wellbore storage effect was 5 hrs (Table 4.1 in Lee, 1982).

Table 2
Parameters of test data (Lee, 1982)

Parameters	Value, unit	Parameters	Value, unit
Porosity (ϕ)	0.2	Viscosity (μ)	0.8 cp
Flow rate (q)	500 STB/DAY	Formation volume factor (B_o)	1.2 RB/STB
Thickness (h)	56 ft	Radius of well (r_w)	0.3 ft
Total compressibility (C_t)	0.00001 psi^{-1}	Initial pressure (Pi)	3,000 psi

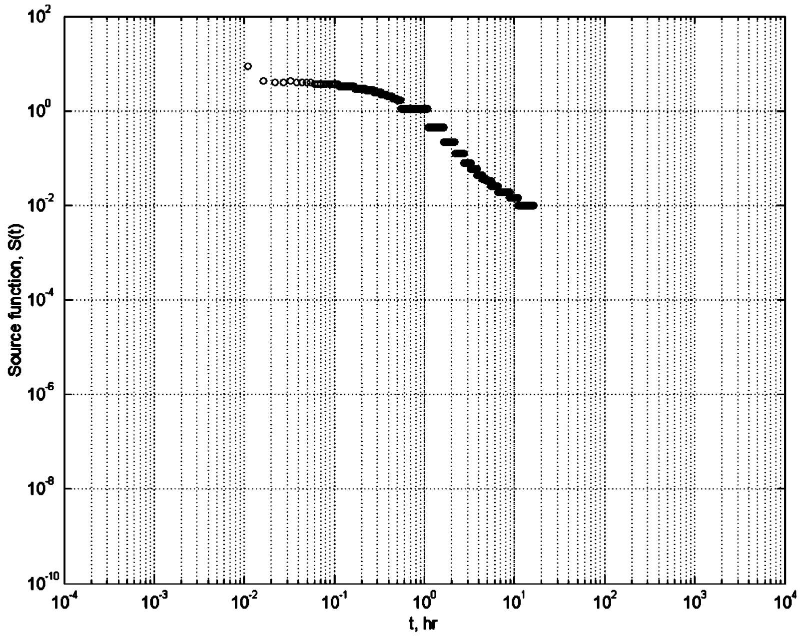

Figure 22. The source function obtained from pressure data in Lee (1982).

When pressure data (Figure 21) with a flow rate of 500 STB/DAY was used, the source function (Figure 22) was obtained by deconvoluting the pressure and flow-rate data based on Eq. (6). The source function obtained (Figure 22) shows that the well had the wellbore storage effect because the source function begins as a horizontal line, becomes a curve, and then tends to coincide with either the infinite line source function or the infinite surface cylinder source function. The source function (Figure 22) from the case shows that the dimensionless wellbore storage coefficient (C_D) is 1,000. The result is the same as that from Lee (1982). In this study, the ending time of the wellbore storage effect from the plot (Figure 22) was estimated to be 5.19 hrs, which is close to the 5 hrs analyzed by Lee (1982).

6. Conclusions

We conclude the following from our study of the characteristics of source functions in early time pressure behavior and their application to pressure test data.

(1) Source functions can be derived by deconvoluting the pressure drop and flow rate, which are available from pressure test data. Source functions can be used to characterize the inner boundary conditions of test wells, such as point source, infinite line source, or infinite surface cylinder source, the wellbore storage effect, and the skin effect. The information is valuable for pressure test analysis.

(2) The pressure function, flow rate, or source function can be derived when two of these three functions are known. The source function is a characteristic of the formation and is independent of the flow rate.

(3) In the log-log plot of the dimensionless source functions versus dimensionless time for different wellbore storage constants, the source functions begin as horizontal

lines and cross over the analytical source function at an early time. At a later time, the ending time of the wellbore storage effect, the source functions coincide with the infinite line source function or infinite surface cylinder source function.

(4) The source functions are almost the same for different positive skin factors (damage effect). For a negative skin factor (stimulation effect), a source function is initially a horizontal line and subsequently coincides with the infinite line source or infinite surface cylinder source functions.

References

Andre, H., and Bennion, D. W. 1970. A transform approach to the simulation of transient gas flow in porous media. *Soc. Petrol. Eng. (SPE) J.* 10:135–139.

Bourdet, D., Ayoub, J. A., and Plrard, Y. M. 1989. Use of pressure derivative in well-test interpretation. *SPE Format. Eval.* 4:293–302.

Clonts, M. D., and Ramey, H. J., Jr. 1986. Pressure transient analysis for wells with horizontal drainholes. *Soc. Petrol. Eng. AIME* 2:215–230.

CMG. 2000. *User's Guide IMEX Advanced Oil/Gas Reservoir Simulator*. Calgary, Alberta, Canada: Computer Modelling Group Ltd.

Gringarten, A. C., and Ramey, H. J., Jr. 1973. The use of source and Green's functions in solving unsteady-state flow petroleum in reservoir. *Soc. Petrol. Eng. AIME J.* 13:285–296.

Kuchuk, F. J. 1990. Applications of convolution and deconvolution to transient well tests. *SPE Format. Eval.* 5:375–384.

Kuchuk, F. J., Carter, R. G., and Ayestaran, L. 1990. Deconvolution of wellbore pressure and flow rate. SPE 13960, *SPE Format. Eval.* 5:53–59.

Lee, J. 1982. *Well Testing*. Dallas, TX: Society of Petroleum Engineers of the AIME.

MATLAB. 2000. *Signal Processing Toolbox for Use with MATLAB User's Guide*. Natick, MA: The Math Works Inc.

Oppenheim, A. V., Schafer, R. W., and Buck, J. R. 1999. *Discrete-Time Signal Processing*. Englewood Cliffs, NJ: Prentice-Hall.

Raghavan, R. 1993. *Well Test Analysis*. Englewood Cliffs, NJ: PTR Prentice-Hall.

Rosa, A. J., and Horne, R. N. 1996. Pressure transient behavior in reservoir with an internal circular discontinuity. *SPE J.* 1:83–92.

Theis, C. V. 1935. The relationship between the lowering of piezometric surface and rate and duration of discharge of wells using ground-water storage. *AIME Trans.* 2:519–524.

van Everdingen, A. F., and Hurst, W. 1949. The application of Laplace transformation to fluid problems in reservoir. *AIME Petrol. Trans.* 189:305–324.

Nomenclature

B	formation volume factor
C, C_t	compressibility, total compressibility
C_D, C_c	dimensionless wellbore storage constant, wellbore storage constant
e	exponential
h	thickness
k	permeability
N	N points, length
n, n', m	sequence
P, P_{wf}, P_{ws}	pressure, bottom hole pressure, shut-in pressure
P_D	dimensionless pressure, defined in Eq. (2) for oil and Eq. (3) for gas
Po, Pi	initial pressure

q	flow rate
q_D	dimensionless flow rate
r	radial distance
r_D	dimensionless radial distance, defined in Eq. (5)
r_w	radius of wellbore
S	source function
S_{il}	infinite line source function
S_{is}	infinite surface cylinder source function
S_{ps}	point source function
s	skin factor
T	temperature
t	time
t_D	dimensionless time, defined in Eq. (4)
Z	real gas deviation factor
η_r	hydraulic diffusivity constant, defined in Eq. (12)
μ	viscosity
τ	integration variable
ϕ	porosity

Subscripts

c	wellbore storage effect
D	dimensionless
i, o	initial
il	infinite line source
is	infinite surface cylinder source
p	polynomial
ps	point source
r	radial coordinate
t	total
w	wellbore
wf	bottomhole
ws	shut-in

Special Function

I_o	modified Bessel function of the first kind of order 0